

# Integrated fracture mechanics approach to analyse fatigue behaviour of welded joints

M. D. Chapetti, J. Belmonte, T. Tagawa and T. Miyata

Current fracture mechanics methods for fatigue assessment, including those that consider thresholds for crack propagation, are based on long crack behaviour. The present work is concerned with an attempt to predict the fatigue strength of welded joints using a fracture mechanics approach that takes into account the fatigue behaviour of short cracks. The methodology estimates the fatigue crack propagation rate as a function of the difference between the applied driving force and the material threshold for crack propagation, which is a function of crack length. The fatigue strength of butt welded specimens stressed transversely was analysed. Experimental results from the literature were used for comparison. Estimations are obtained by using only the fatigue limit and the fatigue propagation threshold for long cracks, and the applied stress distribution along the crack path obtained from simple finite element models. The influence of plate thickness, initial crack length, and reinforcement angle on fatigue strength of butt welded joints was analysed. Results show good agreement with experimental trends. STWJ1425

**Keywords:** welded joints, fatigue, fracture mechanics, short cracks, long cracks

Dr Belmonte is in the Instituto de Investigaciones en Ciencia y Tecnología de Materiales (INTEMA), University of Mar del Plata, J. B. Justo 4302, (B7608FDQ), Mar del Plata, Argentina (mchapetti@fi.mdp.edu.ar). At the time this work was carried out Dr Chapetti, Dr Tagawa and Dr Miyata were in the Department of Materials Science and Engineering, Nagoya University, Nagoya 464-8603, Japan. Dr Chapetti is now in INTEMA. Manuscript received 31 July 2003; accepted 17 September 2003.

© 2004 Institute of Materials, Minerals and Mining.  
Published by Maney on behalf of the Institute.

$\Delta K_{CR}$	extrinsic component of $\Delta K_{thR}$
$\Delta K_{dR}$	microstructural threshold
$\Delta K_{th}$	fatigue crack propagation threshold
$\Delta K_{thR}$	fatigue crack propagation threshold for long cracks
$M_k$	correction factor
$n$	constant
$N$	total fatigue life
$R$	stress ratio (minimum stress/maximum stress)
$t$	plate thickness
$t_0$	reference plate thickness
$w$	weld reinforcement width
$x$	distance from weld toe surface along crack path
$Y$	crack shape parameter
$Y_u$	crack shape parameter for welded joint
$\alpha$	weld reinforcement angle
$\rho$	weld toe radius
$\Delta\sigma$	nominal stress adjacent to welded joint
$\Delta\sigma_e$	fatigue limit (endurance $10^7$ cycles)
$\Delta\sigma_{eR}$	smooth fatigue limit
$\Delta\sigma_n$	nominal applied stress range
$\Delta\sigma_t$	fatigue strength for thickness $t$
$\Delta\sigma_{t0}$	fatigue strength for reference thickness $t_0$
$\Delta\sigma_{th}$	threshold stress range for crack propagation
$\sigma_u$	ultimate tensile strength
$\sigma_{ys}$	yield strength
$\Delta\sigma(x)$	local applied stress range
$\sigma_{yy}(x)$	non-uniform stress field calculated along notch bisector, without considering presence of crack

## INTRODUCTION

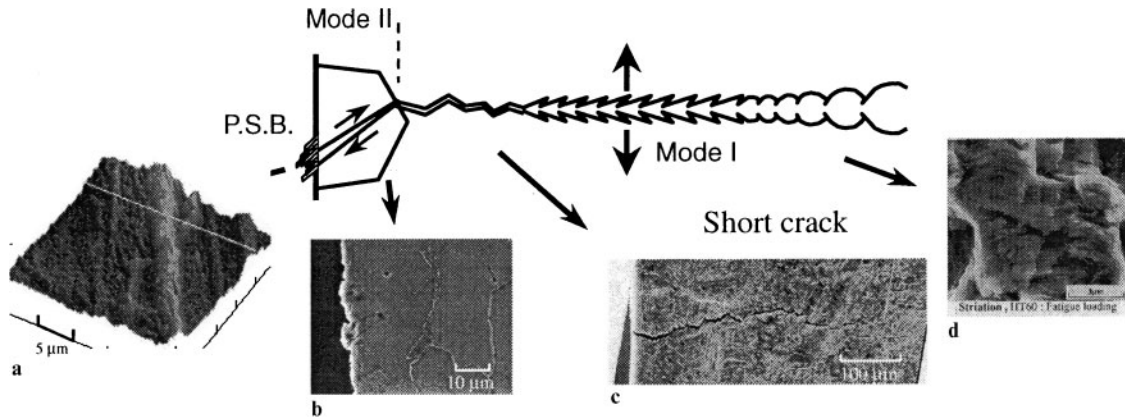
### Mechanical fatigue of metallic materials

Mechanical fatigue of metallic materials can be categorised into the following discrete yet related phenomena<sup>1-3</sup> (see Fig. 1): (i) initial cyclic damage in the form of cyclic hardening or softening due to the surface strain concentration effect; (ii) creation of initial microscopic crack (microcrack initiation); (iii) microcrack propagation to form a (engineering sized) detectable crack (macrocrack initiation); (iv) subsequent macrocrack propagation (macrocrack growth); and (v) final failure or instability. Figure 1 shows photographs with examples of the damage involved in each of steps (i)–(iv) above as found in low carbon steels: part *a* shows extrusions due to persistent slip bands, *b* a cross-section of a microcrack nucleated in a ferrite–pearlite microstructure and arrested at the first grain boundary, *c* a short crack, and *d* an example of striations due to fatigue crack propagation of a long crack.

According to the above definition, microcrack propagation covers the total short crack regime (cracks for which the crack closure effect is not fully developed). In engineering terms, the first three steps are considered as macrocrack initiation, that is, the initiation fatigue life of a material without cracklike defects is defined as the number of cycles necessary to create a detectable crack of length about 0.5–1 mm, a length range similar to that usually observed for the transition between short and long cracks

## LIST OF SYMBOLS

$a$	crack length
$a_f$	final crack length
$a_i$	initial crack length
$a_{np}$	length of non-propagating crack
$da/dN$	crack propagation rate
$A, C, m$	environmentally sensitive material constants
$d$	microstructural dimension (e.g. grain size)
$h$	weld reinforcement height
$k$	material constant that takes into account development of $\Delta K_C$
$k_{tx}$	stress concentration at given distance $x$ from weld toe surface
$\Delta K$	applied stress intensity factor range
$\Delta K_C$	extrinsic component of $\Delta K_{th}$



*a* initial cyclic damage in form of cyclic hardening or softening, e.g. persistent slip bands; *b* microcrack initiation; *c* microcrack propagation leading to initial engineering sized (0.5–1 mm) flaw; *d* subsequent macroscopic propagation until final failure or instability

## 1 Mechanical fatigue of materials without cracks or cracklike defects

(crack length at which the crack closure effect is fully developed). This definition supports the strongly held belief that the fatigue life of a material without cracklike defects is mainly determined by fatigue crack initiation life. However, if the fatigue crack initiation life is defined by the first two steps, i.e. the microcrack propagation (or short crack propagation) step is included in the propagation period, it is possible to find instances for which the fatigue life is mainly given by the fatigue crack propagation life.<sup>4–6</sup> Thus it is important to take into account the crack length to define clearly the transition between crack initiation and crack propagation periods.

### Fatigue of welded joints

An important consequence of the geometric stress concentrations associated with most welded joints, the severity of which is usually compounded by the presence of welding flaws, is that fatigue cracks readily initiate and the life is dominated by fatigue crack growth.<sup>7–9</sup> This accounts for the drastic reduction in fatigue life resulting from the presence of a weld. It also explains why fracture mechanics is so relevant to the fatigue assessment of weldments.

There exist several calculation methods for fatigue life of welded joints, including the nominal stress method, hot spot method, notch stress method, local strain method, and fracture mechanics methods. Most of these methods are currently already either officially standardised,<sup>10,11</sup> or at least in internationally accepted recommendations.<sup>9</sup> This renders them more usable and acceptable in design work. However, there still exists a dominance of the traditional nominal stress method, which has been prevailing for over 35 years in the fatigue design of welded structures.

To ensure that the full effect of the three key features dominating the fatigue life of welded joints (geometric stress concentrations, welding flaws, and residual stresses) are allowed for in design, most fatigue design rules consist of series of  $\Delta\sigma$ – $N$  curves based on data obtained from constant amplitude fatigue tests on actual weldments,<sup>7–9</sup> in which use is usually made of the commonly employed classification method of specifying design curves in terms of the fatigue strength at a given number of cycles (e.g.  $2 \times 10^6$  or  $10^7$ ). Since the stress concentration effect of the welded joint geometry is included,  $\Delta\sigma$  refers to the nominal stress adjacent to the weld. Furthermore, to allow for the influence of residual stresses, the full stress range is used. The  $\Delta\sigma$ – $N$  curves are used in conjunction with Miner's rule to design structures subjected to variable amplitude loading. Traditionally high reliability strength values ( $\Delta\sigma$ – $N$  curves) are presented in the design codes, e.g. British

Standard<sup>10</sup> 97.7%. The IIW recommendation<sup>9</sup> gives almost all fatigue resistance data as characteristic values, which have a survival probability of at least 95%, calculated from a mean value of two sided 75% confidence level.

### Traditional fracture mechanics approach applied to welded joints

Among all the available methods, the fracture mechanics method permits more precise calculation to be carried out and is a good example of current possibilities when dealing with crack assessment procedures.

If the fatigue life of the welded joint consists mainly of crack growth, and the initial cracklike defects are as long as 0.5–1 mm, the  $\Delta\sigma$ – $N$  curve can be calculated by integrating the Paris crack growth law and using the usual fracture mechanics terminology for long cracks<sup>12</sup>

$$\frac{da}{dN} = C\Delta K^m \quad \dots \quad (1)$$

where the constants  $m$  and  $A$  are obtained from long crack fatigue behaviour, and the stress intensity factor range  $\Delta K$  is given by the following general expression<sup>12</sup>

$$\Delta K = Y\Delta\sigma_n(\pi a)^{1/2} \quad \dots \quad (2)$$

where  $Y$  is a function of crack size and shape and of loading.

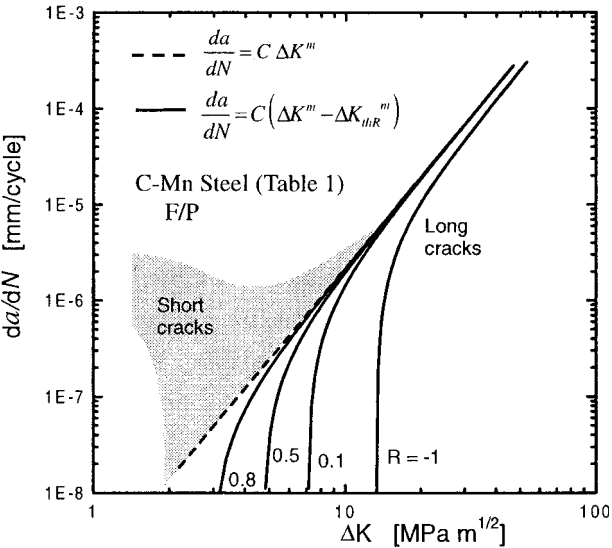
From equations (1) and (2), and integrating from an initial crack length  $a_i$  to a final crack depth  $a_f$ , the resulting  $\Delta\sigma$ – $N$  curve for a given stress ratio  $R$  is predicted to be

$$\Delta\sigma_n^m N = A \quad \dots \quad (3)$$

According to this expression, the  $\Delta\sigma$ – $N$  curve is linear on a log–log basis with a slope  $m$  equal to that of the Paris law. As a consequence of this, most design  $\Delta\sigma$ – $N$  curves for welded joints are taken to be parallel, with a slope compatible with the fatigue crack law for the material. Since  $m$  is approximately 3 for most materials,  $\Delta\sigma$ – $N$  curves with slopes of 3 are widely adopted.<sup>9–11,13</sup>

### Threshold for fatigue propagation of long cracks

An effect of stress ratio  $R$  (minimum to maximum applied stress) is evident at growth rates less than  $5 \times 10^{-6}$  mm cycle<sup>–1</sup> (Ref. 14). Below this propagation rate the material exhibits a deviation from the Paris relationship (equation (3)) used by various workers<sup>15–17</sup> to describe crack growth in welds. Thus a simple linear relationship between stress intensity and growth rates on logarithmic scales is only accurate when the joints are subjected to high stress ratio or high nominal loads producing crack growth



2 Examples of fatigue crack propagation rates as function of applied  $\Delta K$ , estimated using equation (4) for several  $R$  values

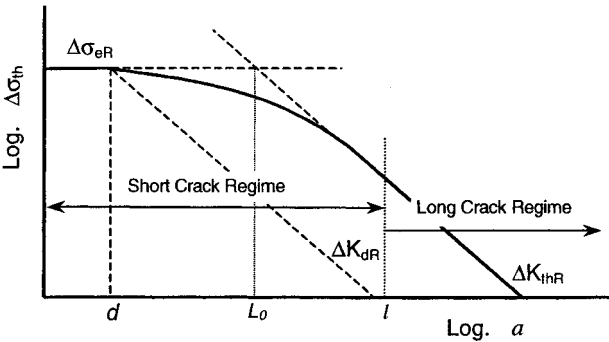
rates greater than  $10^{-5}$  mm cycle $^{-1}$ . A possible simple alternative to the linear relationship, among others, is as follows<sup>14,18</sup>

$$\frac{da}{dN} = C(\Delta K^m - \Delta K_{thR}^m) \dots \dots \dots (4)$$

where  $\Delta K_{thR}$  is a function of stress ratio, and represents the effective resistance of the material to fatigue crack propagation. Figure 2 shows results from equation (4) (bold lines) for different  $R$  values using data from Table 1 for a low carbon steel with a ferrite–bainite microstructure. The broken line shows the linear relation (equation (1)). As the stress ratio  $R$  increases, the curve given by equation (4) tends towards that given by the linear relation. For high effective stress ratios (given by high applied stress ratio or tensile residual stresses), for which the threshold for long cracks in steels varies from 2 to 4 MPa m $^{1/2}$ , both curves show the same trend. Even though equation (1) gives conservative estimations, it cannot be used to analyse, for instance, the influence of residual stresses: the lower the residual stress, the higher the threshold for fatigue crack propagation and therefore, the greater the difference between the curves given by equations (1) and (4).

Implications of short crack regime

Another important factor that should be taken into account is that short cracks usually show lower threshold levels and higher propagation rates than long cracks when considering the same applied driving force  $\Delta K$  (see Fig. 2). The short crack effect can be observed until a crack length is reached that depends on the effective stress ratio  $R$ , and can be in the range 0.5–1 mm for structural steels.<sup>1–3</sup> Previous investigations on fatigue of welded joints have observed an initial cracklike defect depth of about 10–120  $\mu$ m,<sup>19</sup> 20–150  $\mu$ m,<sup>20</sup> or 10–400  $\mu$ m,<sup>21</sup> according to the welding conditions and applied quality control. Radaj and Sonsino<sup>22</sup> have recommended an initial crack size  $a_i$  = 0.1–0.25 mm for



3 Kitagawa–Takahashi diagram showing threshold stress for fatigue crack propagation as function of crack length

life predictions in welded structures. Such defect depths clearly fall within the short crack regime, thus short crack behaviour should be taken into account in any analysis in which the initial crack length is in the range 20–400  $\mu$ m. The influence of short cracks could be more important when considering improvement of fatigue strength via residual stress methods, such as toe peening, the influence of which prevails to a depth similar to half the diameter of the indenter.<sup>7</sup> Previous work<sup>14,23</sup> has shown that when equation (4) is applied without taking into account the short crack effects, fatigue limits and fatigue strength at low stress levels are overestimated. However, the overestimation was attributed to incomplete stress relief and the influence of short crack behaviour was not taken into account.

Threshold for fatigue propagation of short cracks

The effect of crack size on fatigue crack propagation threshold can be described conveniently via the Kitagawa–Takahashi plot relating the threshold stress to the crack size, as shown in Fig. 3. For long cracks (having a length greater than that at which crack closure is fully developed), the fatigue crack propagation threshold decreases with increasing crack size.<sup>5,24–26</sup> The threshold for long cracks is defined in terms of the threshold value of the stress intensity factor range  $\Delta K_{thR}$ , thus long cracks in constant amplitude loading can only grow via fatigue if the applied stress intensity factor range  $\Delta K$  is greater than  $\Delta K_{thR}$ . In Fig. 3, a log  $\Delta\sigma$  versus log  $a$  plot, the threshold for fatigue crack propagation follows a line with slope  $-1/2$  (see equation (2)). As the crack length decreases,  $\Delta\sigma$  increases, and tends to  $\infty$  when the crack length tends to zero. However, there is a practical limit given by the fatigue limit (a function of stress ratio). For a microstructurally short crack (the crack length is of the order of the microstructural dimensions) initiated from a smooth surface the fatigue limit at a given stress ratio  $\Delta\sigma_{eR}$  defines the critical nominal stress range necessary for continued crack growth (microstructural threshold). In the short crack regime the threshold is below  $\Delta\sigma_{eR}$  and  $\Delta K_{thR}$ . The surface strain concentration effect and the development of crack closure govern the threshold level in this regime.<sup>26–28</sup> As a result of the limitation of the fatigue limit (microstructural threshold), the threshold for fatigue crack propagation in terms of the stress intensity factor decreases as the crack length decreases in the short crack regime ( $a < 0.5$ –1 mm).

Table 1 Material chemical composition and mechanical properties of material (C–Mn steel)

Microstructure	C	Si	Mn	P	S	$\sigma_{ys}$ , MPa	$\sigma_u$ , MPa	$d$ , mm	$\Delta\sigma_e$ ( $R=0.1$ ), MPa	$\Delta K_{thR}$ , MPa m $^{1/2}$	$C$	$m$
Ferrite–pearlite	0.11	0.2	0.38	0.013	0.018	286	472	0.028	360	7.6–5.7 $R$	$1.526 \times 10^{-9}$	3.15
Bainite–martensite	0.08	0.21	1.5	0.004	0.003	532	740	0.05	520	9 ( $R=0.1$ )	$1.15 \times 10^{-9}$	3.15

Thus, in those instances in which the initial crack length lies in the short crack regime, short crack behaviour should be considered. If it is not, overestimations could be obtained.

## Objectives

Fracture mechanics methods to estimate the fatigue crack propagation behaviour in structures and components, together with damage tolerant design procedures (allowance of existing cracks in the structure), are currently powerful tools for life assessment, structural integrity analysis, and life extension. However, fracture mechanics methods are not fully included in rules and recommendations for design of welded components. Besides, due to the assumption of the existence of relatively long initial cracklike defects, the short crack effect is not considered when analysing the fatigue behaviour of welded joints. Modern technology has improved the quality of welded joints and maximum initial cracklike defect lengths of about 0.1 mm can be obtained,<sup>19</sup> so that for such cases the short crack effect should be included when using fracture mechanics approaches to estimate fatigue crack propagation lives and fatigue endurance.

Verreman and Nie<sup>29</sup> found that the microcrack initiation life is a small fraction of the total fatigue life (an average of 6%), and that the number of cycles necessary to create a crack 0.5 mm in length is 25–50% of the total fatigue life and can be termed the 'short crack propagation life'. If the total fatigue life of a weld joint is estimated as the number of cycles required to propagate a long crack (e.g. 0.5 mm) to fracture, the estimation will certainly be conservative in those joints where the initial crack length is about 0.1–0.2 mm, and a crack initiation life should be added to the result. However, instead of considering crack initiation life, which is almost unpredictable in welded joints, it would be possible to obtain more accurate estimations by including the short crack propagation period in the crack propagation life estimation.

The present work is concerned with an attempt to predict the fatigue strength of welded joints via a fracture mechanics approach that includes the fatigue crack propagation threshold for both short and long cracks. The methodology,<sup>30</sup> previously developed to analyse the short crack behaviour, estimates the threshold for fatigue crack propagation as a function of crack length  $\Delta K_{th}$ , and the fatigue crack propagation rate as the difference between the applied driving force  $\Delta K$  and  $\Delta K_{th}$ , as follows

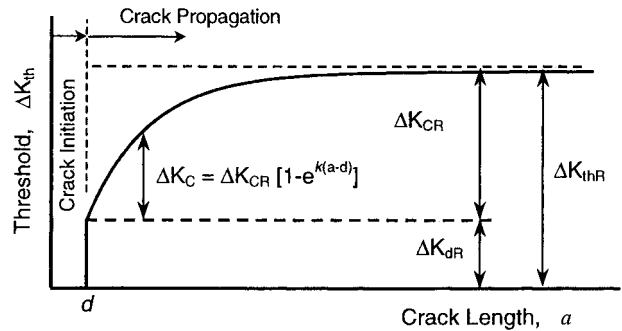
$$\frac{da}{dN} = C(\Delta K^m - \Delta K_{th}^m) \quad (5)$$

In equation (4) the threshold for crack propagation is constant for a given  $R$ , but in equation (5) it is a function of crack length.

The fatigue strength of butt welded specimens stressed transversely was analysed. Experimental results from the literature were used for comparison. The influence of plate thickness, initial crack length, and reinforcement angle on fatigue strength was also estimated.

## FRACTURE MECHANICS APPROACH

Equation (5) states that the difference between the total applied driving force defined by the applied stress intensity factor range for a given geometrical and loading configuration  $\Delta K$  and the threshold for crack propagation  $\Delta K_{th}$  defines the effective driving force applied to the crack. This concept is the basis of the resistance curve method.<sup>26,27</sup> If the short crack effect is considered, according to Fig. 3 the variation of the propagation threshold should be known as a function of crack length. In a previous study<sup>30</sup> an expression for estimating the threshold for fatigue crack propagation as a function of crack length was obtained using only the plain fatigue limit  $\Delta \sigma_{eR}$ , the threshold for



4 Threshold curve defined by equation (6) in terms of stress intensity factor range

long cracks  $\Delta K_{thR}$ , and the microstructural characteristic dimension  $d$  (e.g. grain size). The expression was defined from a depth given by the position  $d$  of the strongest microstructural barrier that defines the smooth fatigue limit (e.g. first grain boundary). Figure 1b shows an example of a cross-section of a crack initiated in a ferritic low carbon steel and arrested by the first grain boundary, found in a specimen tested for  $10^7$  cycles at a nominal stress level 10 MPa lower than the fatigue limit. A microstructural threshold for crack propagation  $\Delta K_{dR}$  is defined by the plain fatigue limit  $\Delta \sigma_{eR}$  and the position  $d$  of the strongest microstructural barrier (see Fig. 3). A total extrinsic threshold for crack propagation  $\Delta K_{CR}$  is then defined by the difference between the crack propagation threshold for long cracks  $\Delta K_{thR}$  and the microstructural threshold  $\Delta K_{dR}$ . The development of the extrinsic component is considered to be exponential and a development parameter  $k$  is estimated as a function of the same microstructural and mechanical parameters used to define the material threshold for crack propagation. The material threshold for crack propagation as a function of the crack length  $\Delta K_{th}$  is then defined as

$$\begin{aligned} \Delta K_{th} &= \Delta K_{dR} + (\Delta K_{thR} - \Delta K_{dR}) \{1 - \exp[-k(a-d)]\} \\ &= Y \Delta \sigma_{th} (\pi a)^{1/2} \quad (a \geq d) \end{aligned} \quad (6)$$

where  $\Delta K_{dR}$  and  $k$  are given by

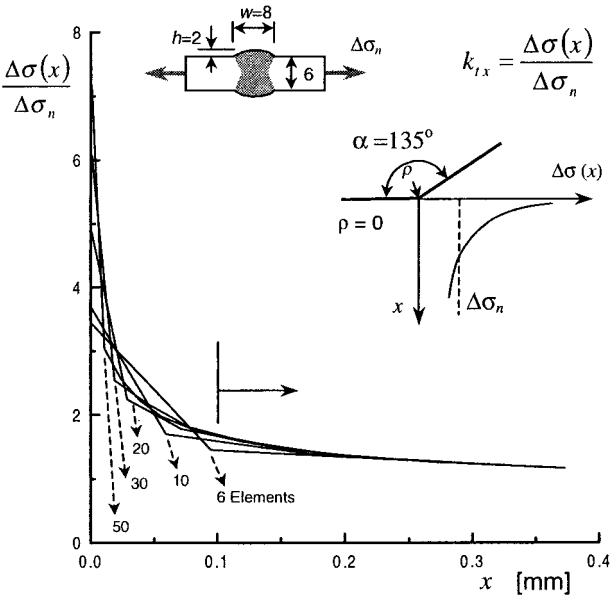
$$\Delta K_{dR} = Y \Delta \sigma_{eR} (\pi d)^{1/2} \quad (7)$$

$$k = \frac{1}{4d} \frac{\Delta K_{dR}}{(\Delta K_{thR} - \Delta K_{dR})} \quad (8)$$

Figure 4 shows schematically the threshold curve given by equation (6) in terms of the stress intensity factor range. For a crack length  $a=d$ ,  $\Delta K_{th} = \Delta K_{dR}$ , and  $\Delta K_{th}$  tends to  $\Delta K_{thR}$  for long cracks. The expression defined to estimate the material threshold for crack propagation as a function of the crack length allows the definition of a crack initiation period as the number of load cycles necessary to initiate a crack of depth  $d$  (microcrack initiation), from which the crack propagation behaviour can be analysed. This is appropriate for a material free of cracks or cracklike defects. In a welded joint the presence of defects usually renders the crack initiation period irrelevant, and the initial crack length for the crack propagation period will be given by the maximum sized cracklike defect.

## ESTIMATION OF FATIGUE STRENGTH OF BUTT WELDED JOINTS

The present work is concerned with an attempt to predict the fatigue strength of welded joints via a fracture mechanics approach that allows analysis of the fatigue propagation of initial cracks as small as a microstructural characteristic dimension. To achieve this, the fatigue strength of butt welded specimens under transverse stress was analysed. The approach was also applied to analyse the



5 Stress distributions calculated using different finite element sizes: number of elements along half thickness is indicated

influence of some geometrical parameters involved in the definition of the fatigue strength of the weld joint, such as the influence of plate thickness, initial crack length, and reinforcement angle. Fatigue strengths recommended by the IIW<sup>9</sup> for the associated weld joints are considered as a lower limit (corresponding to a survival probability of at least 95%), and an experimental results map from Ref. 13 is considered to represent the observed scatter. Recent experimental results for fatigue strength of butt welds obtained by Taylor *et al.*<sup>31</sup> for the same type of joint were also used for comparison. In the work of Taylor *et al.* simple butt welds of thickness 12.5 mm were made using conventional manual metal arc welding, and tested. The material used was a low carbon steel En2b (0.2 wt-%C, 0.8 wt-%Mn, yield strength 309 MPa). All specimens were fully stress relieved at 600°C immediately before testing, and fatigue tests were carried out at a frequency of 50 Hz and  $R=0.1$ . Experimental results for the influence of the reinforcement angle on fatigue limit of butt welds from Ref. 7 were also used.

Estimation of applied driving force

The applied driving force is related to the nominal stress range and crack length by equation (2), in which the parameter  $Y$  is a function of crack length, component geometry, and type of loading. It has been proposed by Maddox<sup>32</sup> that the function  $Y$  for a welded joint can be written as

$Y = M_k Y_u \dots \dots \dots (9)$

where  $Y_u$  is the corresponding value of  $Y$  for the same crack geometry in a plate with no weld, and  $M_k$  is a correction factor that takes into account the effect of joint geometry and weld profile. Thus, for a welded joint, it follows that

$\Delta K = M_k Y_u \Delta \sigma (\pi a)^{1/2} \dots \dots \dots (10)$

Hence, given that the value of  $Y_u$  for standard crack shapes is already known, the problem is to calculate  $M_k$ . The method for this was based on a superposition approach using the stress distribution in an uncracked plate along the expected crack path. Even though the method is only approximate, it is considered to be satisfactory for use in the study of variables for relatively similar joint types, since for such joints the errors are likely to be similar.

However, a more accurate estimation was carried out in the present work, using the superposition and the weight function methods and the following solution for a through thickness crack in a finite plate under tension loading<sup>33</sup>

$$\Delta K = \frac{2}{\sqrt{\pi}} \int_0^a \left[ \frac{\Delta \sigma_{yy}(x)}{\sqrt{a}} \left( \frac{3.52 (1 - \frac{x}{a})}{(1 - \frac{x}{l})^{3/2}} - \frac{(4.35 - 5.28 \frac{x}{a})}{(1 - \frac{x}{l})^{1/2}} + \left\{ \frac{1.3 - 0.3 (\frac{x}{a})^{3/2}}{[1 - (\frac{x}{a})^2]^{1/2}} + 0.83 - 1.76 \frac{x}{a} \right\} \left[ 1 - (1 - \frac{x}{a}) \frac{a}{l} \right] \right) \right] dx \quad (11)$$

The non-uniform stress field  $\sigma_{yy}(x)$  was estimated using finite element models constructed using the FINAS code.<sup>34</sup> In all instances plate thickness was 6 mm. Eight node quadratic elements were used in a static, elastic analysis. Figure 5 shows stress distributions estimated from the model with different numbers of elements along the crack path. It can be observed that 20 elements along half the plate thickness (3 mm) are sufficient to obtain convergence for the stress distribution for depths greater than 0.1 mm. However, about 30 elements were used for all models to ensure that an accurate stress distribution was obtained.

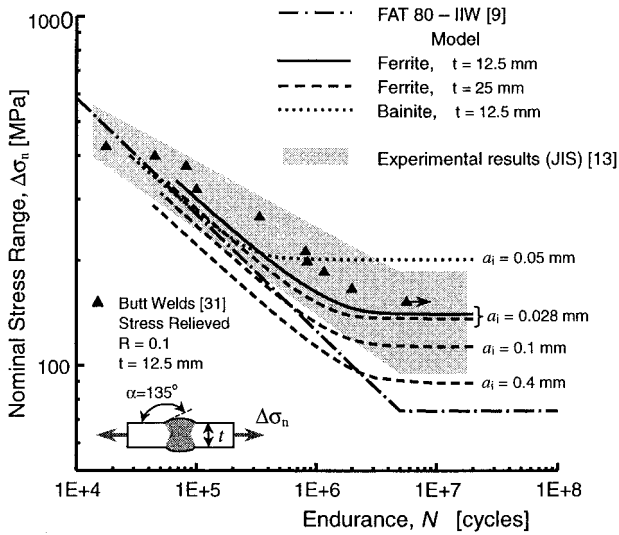
The weld toe was modelled as a sharp corner, so that theoretical elastic stresses near to the surface would tend to infinity. This is acceptable as cracklike initial defects exist almost continuously along the weld toe. Therefore, the stresses at the surface are not required, but rather the stress from a depth equal to the initial crack length considered, the value of which is usually greater than 0.1 mm. To confirm this hypothesis, models with 135° reinforcement angle and different toe root radii were constructed. Table 2 gives the stress concentration obtained at different depths  $k_{tx}$  from the toe root (*see also* definition in Fig. 5). It can be observed that  $k_{tx}$  does not depend on the notch root radius when  $x > 0.2 \rho$ . The limit for the validity of this assumption is defined by the italic numbers in Table 2. Because it seems reasonable to consider a value of 0.1 mm as a minimum initial crack length for weld joints, the influence of notch root radius seems to have no important effect on the applied stress distribution for notch root radii less than 0.5 mm. A greater toe radius would give lower stress concentrations, so that in such instances the assumption would be conservative, or the toe radius could be readily included in a simple and coarse finite element model.

To analyse the influence of plate thickness on fatigue strength of the joints, the stress distributions corresponding to different thicknesses were estimated considering the stress distribution obtained for a 6 mm thickness plate, from which a stress distribution parameterised with the plate thickness was obtained. In this procedure, the stress concentration factor associated with the joint is constant for any plate thickness, but it is possible to analyse the influence of the stress gradient near the weld toe on fatigue

Table 2 Stress concentration calculated at different depths from toe root along crack path for different toe radii

$\rho, \text{ mm}$	$k_{tx}$ at $x$ value of					
	1 mm	0.5 mm	0.25 mm	0.1 mm	0.05 mm	0.028 mm
1	0.92	1.06	1.25	1.47	1.57	1.65
0.5	0.92	1.06	1.28	1.62	1.84	1.99
0.25	0.92	1.06	1.28	1.66	2.02	2.29
0.1	0.92	1.06	1.27	1.66	2.07	2.48
0.05	0.92	1.06	1.26	1.65	2.12	2.51
0	0.92	1.06	1.26	1.65	2.09	2.46

Butt weld reinforcement geometry:  $\alpha=135^\circ$ ;  $t=6 \text{ mm}$ ;  $w=6 \text{ mm}$ ;  $h=2 \text{ mm}$ . Minimum element size near notch root 0.025 mm.



6 Fatigue lives for butt welds

strength, which is in turn influenced by the reinforcement angle and the plate thickness.

### Estimation of fatigue crack propagation threshold

In the present work the fatigue properties of two C-Mn steels having ferrite-pearlite and bainite-martensite microstructures were used. Microstructural dimensions, plain fatigue limit, and threshold for long cracks were experimentally measured according to ASTM standards<sup>35,36</sup> (see Table 1). The propagation threshold as a function of crack length in terms of the stress intensity factor range ( $\Delta K_{th}$  versus  $a$ ) or the threshold stress ( $\Delta \sigma_{th}$  versus  $a$ ) was estimated using equations (6)–(8) for  $R=0.1$ .

### Estimation of fatigue strengths

The basic concept used in the present work is that the effective driving force applied to the crack is given by the difference between the total applied driving force defined by the applied stress intensity factor range for a given geometrical and loading configuration  $\Delta K$ , and the threshold for crack propagation as a function of crack length  $\Delta K_{th}$ . Equations (10) and (6) are used to estimate  $\Delta K$  and  $\Delta K_{th}$  respectively. Finally, the fatigue crack propagation life is estimated by integrating equation (5) over a given crack length. The initial crack length  $a_i$  is defined by the largest defect present at the weld toe. Failure was assumed to occur at a final crack length defined as half the plate thickness. If the initiation period is disregarded, the procedure outlined above results in total fatigue lives.

Figure 6 shows some estimated  $\Delta \sigma_n$ - $N$  curves, the experimental results from Ref. 31 for the same type of joint ( $R=0.1$ , stress relieved), the IIW design curve for similar weld joints with the worst quality (FAT 80),<sup>9</sup> which represent the lower limit for experimental fatigue life data, and a region where experimental results are usually observed for the same type of joint,<sup>13</sup> which represents the associated scatter band. Estimations were made for applied  $R=0.1$ , residual stress relieved, final crack length  $a_f=t/2$ , and without misalignments. Among the estimated results is the  $\Delta \sigma_n$ - $N$  curve for the base material (ferrite-pearlite microstructure, see Table 1),  $t=12.5$  mm, and  $a_i=d=0.028$  mm (average grain size). Good agreement can be observed with the experimental results obtained by Taylor *et al.*<sup>31</sup> Estimated values are below experimental values for all fatigue lives. Broken lines correspond to a  $\Delta \sigma_n$ - $N$  curve estimated for  $t=25$  mm and different initial crack lengths  $a_i=0.028$ , 0.1, and 0.4 mm. Finally, the dotted line corresponds to a  $\Delta \sigma_n$ - $N$  curve estimated using

the material parameters for a bainite-martensite microstructure (see Table 1). Because toe cracks usually nucleate at heat affected zones, where the microstructure has enhanced fatigue properties, this curve can be considered as an estimation of the upper limit of the possible results for the analysed joint. A small thickness and a very short initial crack were selected for that reason. Conversely, the broken  $\Delta \sigma_n$ - $N$  curve estimated for ferrite-pearlite microstructure steel,  $t=25$  mm, and  $a_i=0.4$  mm can be considered as a lower limit. It can be seen that the two limits delineate the total region within which experimental results are usually observed. The lower limit is also very close to the IIW design curve, which represents the lower limit for experimental fatigue life data observed for a given type of joint.

The results (and the model itself) contradict the general opinion that fatigue strength of welded structures is independent of static strength. This is not entirely true. Fatigue test results are presented as  $\Delta \sigma_n$ - $N$  curves, in which the effects of different static strength levels are hidden by the variation in fatigue strength due to the main influences of initial crack length and residual stresses. To discern the relevant differences, statistical methods are required.

It is worth noting that all estimations were made for  $R=0.1$ , and residual stresses and misalignments were not considered. The influence of residual stresses should be analysed together with an appropriate set of experiments to understand the redistribution and relaxation processes involved when the joints are subjected to cyclic loading and the crack propagates. However, it is obvious from the applied model that if residual stresses were considered and relaxation processes were neglected, all estimated curves would decrease, giving lower fatigue strengths. This is so because tensile residual stresses would increase the applied stress ratio, decreasing the fatigue crack propagation threshold (see resistance curve in Fig. 4). In contrast, the applied driving force would remain constant, so that the effective driving force for crack propagation at a given applied  $\Delta K$  would increase, decreasing the fatigue resistance of the joint.

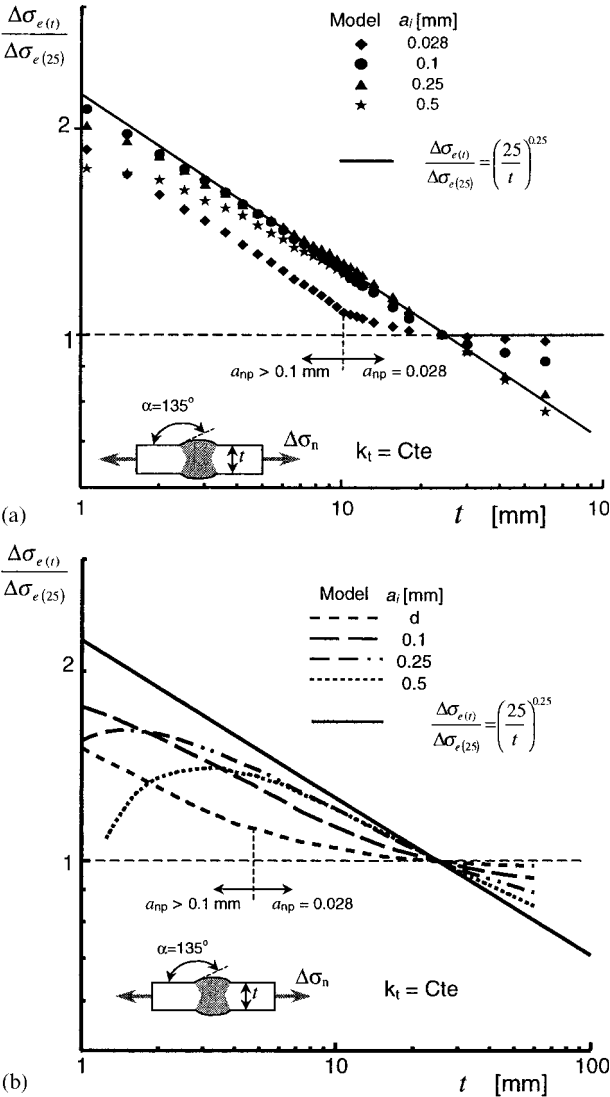
### INFLUENCE OF PLATE THICKNESS IN BUTT WELDS

It has been well established, both theoretically and experimentally, that fatigue endurance decreases when plate thickness increases. Traditionally the thickness effect has been used so that the fatigue strength is reduced for thicknesses greater than a certain limit, usually 25 mm, according to the following expression

$$\Delta \sigma_t = \Delta \sigma_{t0} \left( \frac{t_0}{t} \right)^n \quad (12)$$

where  $n$  is based on test results. The IIW recommendation<sup>9</sup> suggests  $t_0=25$  mm and  $n=0.25$  for butt welds. Gurney<sup>37</sup> states that this rule could be extrapolated back to thinner joints, but also concluded that further work is necessary to confirm the effect.

Figure 7 shows estimated results for the fatigue endurance defined at  $10^7$  cycles as a function of the plate thickness for different initial crack lengths. The correction recommended by the IIW for butt joints is also shown, extrapolated to thicknesses less than 25 mm (broken line). Figure 7a corresponds to fatigue limits estimated using the fatigue crack propagation threshold conditions in terms of stress ( $\Delta \sigma_{th}$ ), whereas for Fig. 7b the propagation threshold curve in terms of the stress intensity factor ( $\Delta K_{th}$ ) was used. Even though the results show a similar general trend in both figures, that is, the fatigue limit decreases with thickness as is usually observed, results from Fig. 7b show notable differences in the influence of the initial crack length on the fatigue limit of thin plates ( $t < 10$  mm). Figure 7a shows that equation (12) could be extrapolated to thicknesses smaller

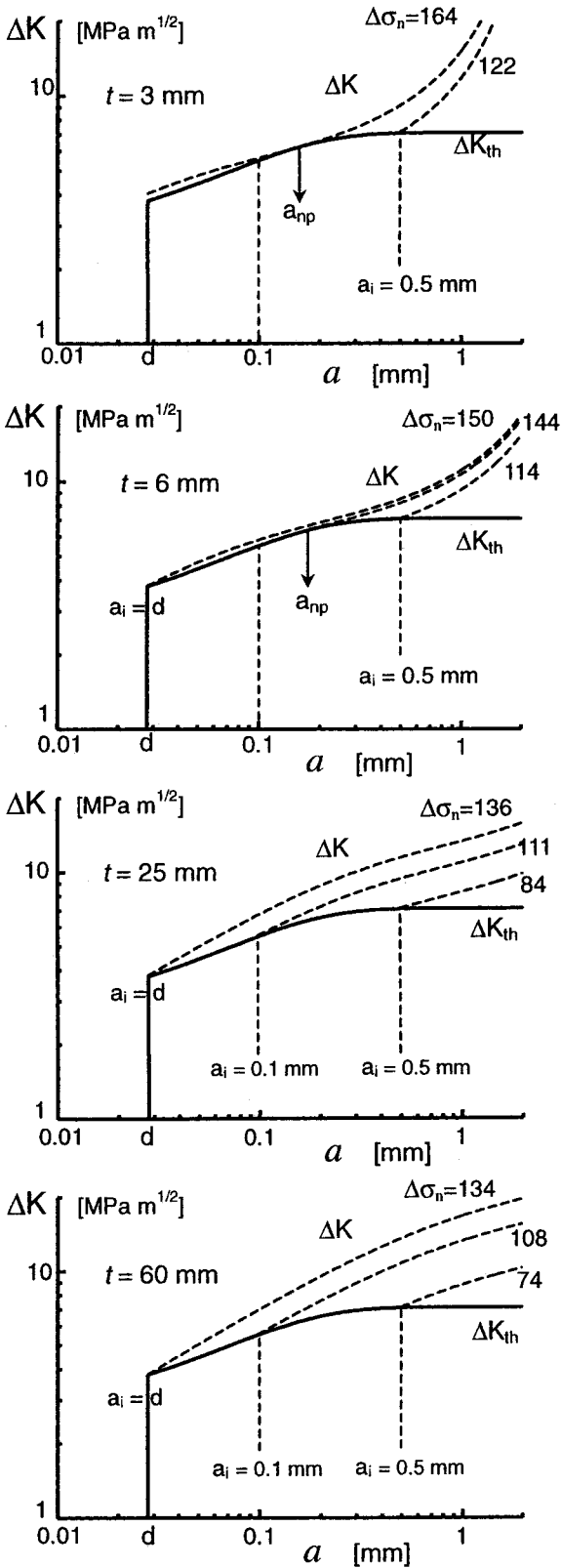


7 Influence of plate thickness on fatigue strength of butt welds (endurance  $10^7$  cycles): estimations are carried out considering  $a$  threshold stress for fatigue crack propagation (see Fig. 2) and  $b$  threshold for fatigue crack propagation in terms of  $\Delta K$  (see Fig. 3)

than 2 or 3 mm, whereas Fig. 7b shows that extrapolation could lead to overestimation of fatigue strength for thicknesses smaller than 6 mm. Figure 7b also shows that an opposite tendency in the relation between fatigue limit and thickness could be found for thin plates ( $t < 6$  mm) when initial crack length is longer than about 0.3 mm. This opposite effect was recently observed experimentally by, for instance, Gustafsson<sup>38</sup> for non-load carrying attachments with 3 and 6 mm plate thickness.

In Fig. 7 the observed thickness effects are related to the effect of stress gradients and initial crack length. Another mechanism that can contribute to the thickness effect is the manufacturing or process history, which can lead to different grain and inclusion sizes and hence different fatigue properties. However, this effect is usually observed to be small in comparison with the effects of gradient and initial crack length on fatigue strength.

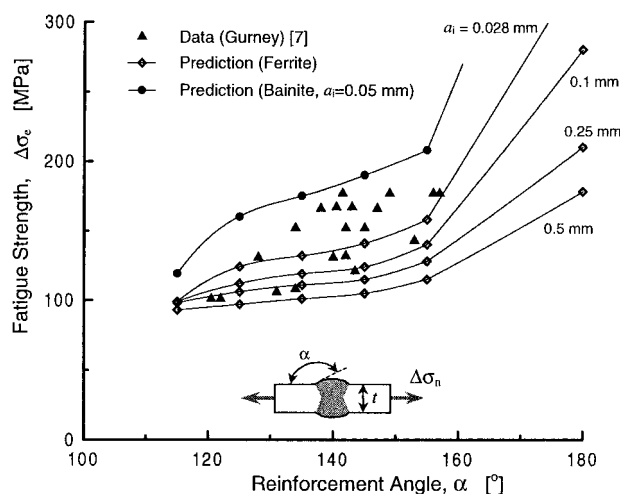
For initial crack lengths smaller than 0.1 mm, as for  $a_i = 0.028$  mm, a smaller exponent appears from a given thickness (about 10 mm in Fig. 7a and 6 mm in Fig. 7b). This is attributed to the fact that the influence of the stress gradient on fatigue limit decreases as the initial crack length decreases. Figure 8 consists of four graphs showing



8 Applied driving force ( $\Delta K$ , broken lines), and threshold for crack propagation ( $\Delta K_{th}$ , solid lines), as function of crack length for four different plate thickness of 3, 6, 25, and 60 mm: nominal stresses  $\Delta\sigma_n$  for each  $\Delta K$  curve correspond to fatigue limit estimated for given initial crack length ( $a_i = d$ , 0.1 mm, or 0.5 mm)

applied driving forces and the threshold for fatigue crack propagation, in terms of the stress intensity factor. Each graph corresponds to a given thickness of 3, 6, 25, or 60 mm. For each graph several applied driving forces are





9 Influence of reinforcement angle on fatigue strength of butt welds

shown, given by the nominal stress level corresponding to the fatigue limit for an initial crack length of 0.028, 0.1, or 0.5 mm. It can be seen that below a given thickness, it could be possible to obtain a non-propagating crack of size in the range 0.08–0.2 mm. This is the reason for the different slope observed in Fig. 7b for  $a_i=0.028$  mm. In this instance, the fatigue limit is given by  $a_i=d=0.028$  mm for thicknesses greater than 6 mm, but it is governed by a non-propagating crack of length about 0.1 mm for thicknesses smaller than 6 mm, and the slope of the relation becomes similar to that for  $a_i=0.1$  mm. The same effect occurs in Fig. 7a where the analysis was carried out in terms of  $\Delta\sigma_{th}$ , but the transition is observed at a plate thickness of about 10 mm. The relative position between the applied driving force distribution and the material crack propagation threshold curve seems to define a thickness range below which the fatigue limit is given by a non-propagating crack of length varying from 0.08 to 0.18 mm. An initial crack length smaller than 0.1 mm is rare in welded joints, so that this occurrence could be difficult to observe in actual cases. However, as will be shown below, this mechanism could be one of the reasons for the low scatter in fatigue strength experimentally observed for small reinforcement angles.

## INFLUENCE OF REINFORCEMENT ANGLE IN BUTT WELDS

Gurney<sup>7</sup> has pointed out that the fatigue strength of butt welds varied widely, from 100 to 180 MPa, for  $R$  values close to zero. It was pointed out that the main reason for these variations seems to be the local shape of the reinforcing cap, especially the angle  $\alpha$  between the reinforcement and the base metal. Figure 9 shows the well known experimental results presented by Gurney, together with results for the estimated fatigue limit as a function of the reinforcement angle for different initial crack lengths. Even though the estimated results seem to be somewhat lower than the experimental results, the trend is well estimated. It is worth noting that the model can explain the reduction in the scatter observed as the reinforcement angle decreases. This is because as the reinforcement angle decreases, the stress gradient near the weld toe increases, and from a given value non-propagating cracks define the fatigue limit. The size of these non-propagating cracks is in the range 0.1–0.2 mm, so that the fatigue limit would be similar for  $a_i=0.028$ , 0.1, and 0.2 mm, as can be observed for  $\alpha=115^\circ$ . This is similar to the results shown in Fig. 8a and b, in which it can be seen that the minimum applied nominal stress range for which a crack could propagate shows almost no influence of  $a_i$  for  $d < a_i < 0.25$  mm.

Figure 9 also shows results obtained using the material data corresponding to a bainite–martensite microstructure and  $a_i=0.05$  mm. It can be observed that the estimated curve falls above the upper limit of the experimental results. The region between the upper (bainite–martensite,  $a_i=0.05$  mm) and lower (ferrite–pearlite,  $a_i=0.5$  mm) estimated curves, which can be considered as an upper and lower limit, respectively, includes all the experimental results.

## CONCLUDING REMARKS

Even though modern technology has improved the quality of welded joints and maximum initial cracklike defect lengths of about 0.1 mm can be obtained, almost no attempts have been carried out previously to analyse the influence of the short crack effect in the definition of fatigue strength of welded joints.

In the present work the fatigue strength of butt welded joints stressed transversely was estimated via a fracture mechanics approach that takes into account the fatigue behaviour of short cracks. In the methodology, developed previously, the fatigue crack propagation rate is estimated as a function of the difference between the applied driving force and the material threshold for crack propagation, which is a function of crack length. The material threshold for crack propagation is estimated for the material involved using its smooth fatigue limit  $\Delta\sigma_{eR}$ , its threshold for long cracks  $\Delta K_{thR}$ , (both for the same  $R$  ratio), and its microstructural characteristic dimension. The applied driving force is calculated for the analysed geometric and loading configuration and for this purpose the applied stress distribution along the crack path is obtained from simple finite element analysis models. Experimental results for butt welds from the literature were used for comparison. The influence of plate thickness, initial crack length, and reinforcement angle on fatigue strength of butt welded joints was analysed and estimations show good agreement with experimental data and trends.

Even though more detailed experimental results should be obtained and extensive parametric studies should be carried out to reach important conclusions about the influence of the geometrical, microstructural, and mechanical parameters involved in the definition of the fatigue behaviour of welded joints, the analysis shows that the present fracture mechanics approach could be capable of describing most of their interactions and providing a powerful tool to estimate the fatigue strength of different weld configurations, including those where short crack propagation should be considered.

## ACKNOWLEDGEMENTS

One of the authors (MDC) wishes to express his thanks for funding provided by CONICET (Consejo Nacional de Investigaciones Científicas y Técnicas), and by Agencia Nacional de Promoción Científica y Tecnológica, Argentina.

## REFERENCES

1. K. S. CHAN, J. LANKFORD and D. L. DAVIDSON: *J. Eng. Mater. Technol.*, 1986, **108**, 20–36.
2. S. SURESH and R. O. RITCHIE: *Int. Met. Rev.*, 1984, **29**, 445–475.
3. K. J. MILLER and E. R. DE LOS RIOS: 'The behaviour of short fatigue cracks'; 1988, London, EGF Publications.
4. D. TAYLOR and J. K. KNOTT: *Fatigue Eng. Mater. Struct.*, 1981, **4**, (2), 147–155.
5. M. D. CHAPETTI, T. KITANO, T. TAGAWA and T. MIYATA: *Fatigue Fract. Eng. Mater. Struct.*, 1998, **21**, 1525–1536.
6. K. TOKAJI, T. OGAWA and Y. HARADA: *Fatigue Fract. Eng. Mater. Struct.*, 1986, **9**, (3), 205–217.
7. T. A. GURNEY: 'Fatigue of welded structures'; 1978, Cambridge, UK, Cambridge University Press.
8. 'AWS structural welding code', 9th edn, American Welding Society, Miami, FL, USA, 1985.



9. A. HOBBACHER: 'Fatigue design of welded joints and components', Doc. XIII-1539-96, International Institute of Welding, Vienna, 1996.
10. 'Fatigue design and assessment of steel structures – code of practice', British Standard BS 7608: 1993.
11. 'Guide on methods for assessing the acceptability of flaws in metallic structures', British Standard BS 7910: 1999.
12. T. L. ANDERSON: 'Fracture mechanics', 2nd edn, 517; 1995, Boca Raton, FL, USA, CRC Press.
13. 'Guideline for fatigue design of steel constructions', Japan Society of Steel Construction (JSSC), Gihodo Ltd, Tokyo, Japan, 1993.
14. I. F. C. SMITH and R. A. SMITH: *Eng. Fract. Mech.*, 1983, **18**, (4), 861–869.
15. F. V. LAWRENCE: *Weld. Res.*, 1973, **52**, 212s–220s.
16. N. T. NGUYEN and M. A. WAHAB: *Eng. Fract. Mech.*, 1996, **55**, (3), 453–469.
17. S. T. LIE and S. LAN: *Int. J. Fatigue*, 1998, **20**, (6), 433–439.
18. I. F. C. SMITH, U. BREMEN and M. A. HIRT: Proc. Conf. 'Fatigue '84', Vol. 3, 1773–1782; 1984, Sheffield, UK, EMAS.
19. I. F. C. SMITH and R. A. SMITH: *Fatigue Fract. Eng. Mater. Struct.*, 1982, **5**, (2), 151–165.
20. E. G. SIGNES, R. G. BAKER, H. D. HARRISON and F. M. BURDEKIN: *Weld. J.*, 1967, **14**, 108–116.
21. F. WATKINSON, P. H. BODGER and J. D. HARRISON: 'The fatigue strength of welded joints in high strength steels and methods for its improvement', Proc. Conf. on 'Fatigue of welded structures', Abington, Cambridge, UK, The Welding Institute.
22. D. RADAJ and C. M. SONSINO: 'Fatigue assessment of welded joints by local approaches'; 1998, Cambridge, UK, Abington Publishing.
23. S. J. MADDOX: 'Some aspects of the influence of residual stresses on the fatigue behaviour of fillet welded joints in steel', Welding Institute Members Report 123, Abington, Cambridge, UK, 1980.
24. K. J. MILLER: *Fatigue Fract. Eng. Mater. Struct.*, 1993, **16**, (9), 931–939.
25. M. D. CHAPETTI, T. KITANO, T. TAGAWA and T. MIYATA: *Int. J. Fatigue*, 1999, **21**, (1), 77–82.
26. A. J. MCEVILY and K. MINAKAWA: *Eng. Fract. Mech.*, 1987, **28**, (5/6), 519–527.
27. K. TANAKA, Y. NAKAI and Y. YAMASHITA: *Int. J. Fract.*, 1981, **17**, (5), 519–533.
28. H. ABDEL-RAOUF, T. H. TOPPER and A. PLUMTREE: *Scr. Metall. Mater.*, 1991, **25**, (3), 597–602.
29. Y. VERREMAN and B. NIE: *Fatigue Fract. Eng. Mater. Struct.*, 1996, **19**, 669–681.
30. M. D. CHAPETTI: *Int. J. Fatigue*, 2003, **25**, (12), 1319–1326.
31. D. TAYLOR, N. BARRETT and L. GABRIELE: *Int. J. Fatigue*, 2002, **24**, 509–518.
32. S. J. MADDOX: *Int. J. Fract.*, 1975, **11**, (2), 221–243.
33. Y. MURAKAMI: 'Stress intensity factors handbook'; 1987, Oxford, UK, The Society of Materials Science/Pergamon Press.
34. Finite Element Non-linear Structural Analysis System (FINAS) code, CRC Research Institute, Inc., Tokyo, 1995.
35. 'Standard practice for conducting force controlled constant amplitude axial fatigue test of metallic materials', Standard ASTM E 466–96, in 'Annual book of American Society for Testing and Materials standards', Vol. 03.01, 532; 2001, West Conshohocken, PA, USA, ASTM.
36. 'Standard test for measurement of fatigue crack growth rates', Standard ASTM E 647–00, in 'Annual book of American Society for Testing and Materials standards', Vol. 03.01, 636; 2001, West Conshohocken, PA, USA, ASTM.
37. T. R. GURNEY: 'Fatigue of thin walled joint under complex loading'; 1997, Cambridge, UK, Abington Publishing.
38. M. GUSTAFSSON: in 'Design and analysis of welded high strength steel structures', 205–224; 2002, Sheffield, UK, EMAS.